Joint Reconstruction and Super Resolution of Hyper-Spectral CTIS Images: *Supplementary Material*

Mazen Mel[1]
mazen.mel@dei.unipd.it
Alexander Gatto[2]
alexander.gatto@sony.com
Pietro Zanuttigh[1]
zanuttigh@dei.unipd.it

[1] Department of Information Engineering
University of Padova
Padova, Italy

[2] Sony Europe B.V.
R&D Center - Stuttgart Laboratory 1
Stuttgart, Germany

1 CTIS Sensor Image Simulation

We use Fourier optics to simulate CTIS sensor images via wave field propagation. Starting from the height map h of the DOE, that has a refractive index $n = 1.5$ and is designed for a reference wavelength $\lambda^* = 550nm$ (it creates a phase shift of π at λ^*), we calculate the phase shift introduced by such DOE on an incident planar wave front:

$$\Phi_\lambda = \frac{2\pi(n-1)}{\lambda} h \tag{1}$$

The PSFs for each wavelength are obtained via:

$$PSF_\lambda \propto \left| \mathcal{F}\{A \cdot e^{i\lambda^* \Phi_\lambda}\} \right|^2 \tag{2}$$

Where $\mathcal{F}$ is the Fourier Transform and A is a binary mask defining the aperture area. The PSF has a large support spanning the total image sensor area and is convolved with ground truth HS cubes f interpolated across the spectral dimension in order to get 200 spectral bands. We sum up all convolution results to end up with a 2D CTIS sensor image:

$$g = \sum_\lambda PSF_\lambda * f_\lambda \tag{3}$$

The obtained sensor image in our simulations has 14 higher diffraction orders surrounding the dispersion-free 0th order in a 3 by 5 formation: each higher diffraction order is basically the ground truth HS cube smeared across the spatial dimension following the projection angle.

© 2022. The copyright of this document resides with its authors.
It may be distributed unchanged freely in print or electronic forms.

2 Real CTIS Prototype

Fig. 1 shows our CTIS setup with two optical paths. The ground truth HS cubes are obtained via a secondary optical path that includes a VariSpec tunable color filter and a monochrome image sensor. We recorded 25 bands for each scene using the VariSpec, the recorded bands span the range from 455*nm* to 695*nm* with a step of 10*nm*. We captured 400 images for training while 95 images were reserved for testing.

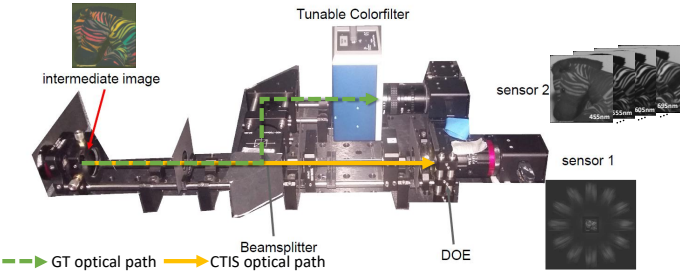

Figure 1: Our real CTIS setup featuring a principal optical path used to capture CTIS sensor images and a secondary path for the ground truth data.

3 HS Video Super-resolution

For this experiment we used different datasets for training and testing the proposed approach. First of all, we trained HSRN on the task of joint HS and SR image reconstruction with $\times 4$ the spatial resolution of the 0th diffraction order on a dataset containing both TokyoTech-31 [3] and CAVE [9] training samples. We then test the network on the Hyper-spectral video dataset [2] in real-time using an NVIDIA A6000 GPU. This dataset contains 31 frames each with a spatial resolution of 752×480 and 33 spectral bands ($400-720nm$). We used only 29 spectral bands as in the training data and resized the ground truth HS cubes to 100×100 in order to simulate CTIS images. The reconstruction time of a cube of size $400 \times 400 \times 29$ is roughly 0.033s. Real-time reconstruction performance is shown in the attached video files (at the original frame rate of 30 fps and slowed down to 2 fps for better visualization). HSRN is able to reconstruct fine object details with good spectral accuracy specially considering that it was trained on different data. The video files are available at: https://lttm.dei.unipd.it/paper_data/HSRN_CTIS/

4 Implementation Details of Competitors

Zimmermann et al. [5]. We changed the *p2cube* layer (reshaping and cropping) to take into account our new DOE design with 14 higher diffraction orders arranged in a 3×5 pattern. The rest of the network is kept as is and all hyper-parameters were also unchanged. The network was trained according to the original paper [5].

Ahlebaek et al. [1]. The authors cropped each higher diffraction order along with the 0th order into individual image each containing a whole projection then stacked them channel-wise and fed the cube to a U-Net architecture. However, the input dimensions used in the original paper are small (250×250) compared to our case were we have some diffraction orders that are dispersed across larger sensor areas (up to 450×450) prompting the padding of the 0th order (which originally has a resolution of 100×100 pixels) by 350×350 pixels. In the modified architecture we removed the third downstream convolution block of the U-Net with 256 filters and added a convolution block with 256 filters in the upstream direction and we included a cropping layer after the last convolution layer that restores the resolution of the 0th diffraction order. Noticed that we modified the network only to account for the new input data dimension preserving at the same time its performance for fair comparison. As for the Expectation Maximization, we used a different implementation than the one provided by [1]: our implementation runs on a GPU and is much faster exploiting shift invariance property of the CTIS system matrix.

References

[1] Mads J Ahlebæk, Mads S Peters, Wei-Chih Huang, Mads T Frandsen, René L Eriksen, and Bjarke Jørgensen. The hybrid approach–convolutional neural networks and expectation maximization algorithm–for tomographic reconstruction of hyperspectral images. *arXiv preprint arXiv:2205.15772*, 2022.

[2] Ajmal Mian and Richard Hartley. Hyperspectral video restoration using optical flow and sparse coding. *Optics express*, 20(10):10658–10673, 2012.

[3] Yusukex Monno, Sunao Kikuchi, Masayuki Tanaka, and Masatoshi Okutomi. A practical one-shot multispectral imaging system using a single image sensor. *IEEE Transactions on Image Processing*, 24(10):3048–3059, 2015.

[4] Fumihito Yasuma, Tomoo Mitsunaga, Daisuke Iso, and Shree K Nayar. Generalized assorted pixel camera: postcapture control of resolution, dynamic range, and spectrum. *IEEE Transactions on Image Processing*, 19(9):2241–2253, 2010.

[5] Markus Zimmermann, Simon Amann, Mazen Mel, Tobias Haist, and Alexander Gatto. Deep learning-based hyperspectral image reconstruction from emulated and real computed tomography imaging spectrometer data. *Optical Engineering*, 61(5):053103, 2022.